

Sorting of mitochondrial and plastid heteroplasmy in Arabidopsis is extremely rapid and depends on MSH1 activity

Amanda K Broz¹, Alexandra Keene¹, Matheus Fernandes Gyorfy¹, Mychaela Hodous¹, Iain G Johnston^{2,3}, Daniel B Sloan¹.

¹Department of Biology, Colorado State University, Fort Collins, CO, USA

²Department of Mathematics, University of Bergen, Bergen, Norway

³Computational Biology Unit, University of Bergen, Bergen, Norway

Author for correspondence:

Amanda K Broz

Email: amandabroz@gmail.com

The authors declare no competing interest.

Key words:

Heteroplasmy, mitochondria, plastid, MutS homolog 1 (MSH1), germline bottleneck

1 **Abstract:**

2 The fate of new mitochondrial and plastid mutations depends on their ability to persist and
3 spread among the numerous organellar genome copies within a cell (heteroplasmy). The extent
4 to which heteroplasmies are transmitted across generations or eliminated through genetic
5 bottlenecks is not well understood in plants, in part because their low mutation rates make these
6 variants so infrequent. Disruption of *MutS Homolog 1 (MSH1)*, a gene involved in plant
7 organellar DNA repair, results in numerous de novo point mutations, which we used to
8 quantitatively track the inheritance of single nucleotide variants in mitochondrial and plastid
9 genomes in Arabidopsis. We found that heteroplasmic sorting (the fixation or loss of a variant)
10 was rapid for both organelles, greatly exceeding rates observed in animals. In *msh1* mutants,
11 plastid variants sorted faster than those in mitochondria and were typically fixed or lost within a
12 single generation. Effective transmission bottleneck sizes for plastids and mitochondria were N
13 ≈ 1 and 4, respectively. Restoring MSH1 function further increased the rate of heteroplasmic
14 sorting in mitochondria ($N \approx 1.3$), potentially due to its hypothesized role in promoting gene
15 conversion as a mechanism of DNA repair, which is expected to homogenize genome copies
16 within a cell. Heteroplasmic sorting also favored GC base pairs. Therefore, recombinational
17 repair and gene conversion in plant organellar genomes can potentially accelerate the
18 elimination of heteroplasmies and bias the outcome of this sorting process.

19

20 **Significance statement:**

21 Mitochondria and plastids play essential roles in eukaryotic life; thus, mutations in these
22 organellar genomes can have severe consequences. In animals, early germline sequestration
23 creates genetic “bottlenecks” providing cell-to-cell variance in mitochondrial mutations upon
24 which selection can act. However, the dynamics of organellar mutations in plants and other
25 organisms that lack early germline segregation remain unclear. Here, we show that sorting of
26 mutations in plant organellar genomes proceeds very rapidly – much faster than in animals. In
27 mitochondria, this process is accelerated by MSH1, a gene involved in recombination and repair
28 of organellar genomes. This suggests that in plants, recombinational repair creates cell-to-cell
29 variance in the frequency of organellar mutations, facilitating selection in the absence of a
30 classical germline bottleneck.

31 **Introduction:**

32 In plants, the genetic system is housed in three different compartments: the nucleus, the
33 mitochondria and the plastids. The products of mitochondrial and plastid genomes perform
34 functions critical for cellular metabolism, including oxidative phosphorylation and
35 photosynthesis. Because organellar genomes are present at high cellular copy numbers,
36 multiple alleles can coexist within a cell, a situation known as heteroplasmy. These variants can
37 create opportunities for selfish competition within cells (1-4) and are of great interest because
38 they are often associated with human disease phenotypes, including inherited disorders due to
39 germline transmission and age-related disorders due to heteroplasmies in somatic tissues (5-7).
40 Because of their important health consequences, the dynamics by which *de novo* mitochondrial
41 point mutations in mammals spread from initially low frequencies to eventually reach fixation
42 (homoplasmy) within a cell have been investigated in detail. Mammalian mitochondrial genomes
43 undergo physical and genetic bottlenecks that increase variance in heteroplasmic alleles among
44 cells, providing a basis for selection (8-10). Bottlenecks in this sense result from a reduction in
45 the effective population size of organellar genomes, which can be due to processes such as
46 drift, preferential organellar DNA amplification, organellar dynamics and/or gene conversion (11-
47 13). The relative size of these bottlenecks can be calculated by comparing variance in
48 heteroplasmic frequencies between mother and progeny (14, 15), and effective mitochondrial
49 bottleneck size (i.e., modelling the heteroplasmy variance generated between generations as a
50 single sampling event) ranges from ~10-30 segregating units in humans (16-19).

51 In contrast to the fairly detailed understanding of mitochondrial heteroplasmy in animal
52 systems, there are fundamental gaps in our knowledge of how mitochondrial and plastid
53 mutational variants sort out in plants. Studies of heteroplasmic frequency in plants have mostly
54 been done with species that show biparental organelle inheritance (20-23), presumably because
55 the exceedingly low point mutation rates in plant organellar genomes (24-26) limit the supply of
56 *de novo* mutations to study. In addition, spontaneous organellar mutations that lead to visible
57 phenotypes in plants (i.e., plastid mutations causing chlorosis or variegation) tend to be severe,
58 and heteroplasmic lines can often only be maintained by vegetative propagation (27, 28). These
59 factors have hampered the study of heteroplasmy dynamics in plants, including the extent to
60 which heteroplasmies are transmitted across generations.

61 The process by which heteroplasmies arise and spread is expected to differ markedly
62 from the accumulation of mutations in the nuclear genome because of three distinguishing
63 characteristics: mode of inheritance, copy number per cell and mutation rate. Organellar
64 genomes show non-Mendelian inheritance, typically characterized by maternal transmission as

65 opposed to the biparental inheritance of nuclear genomes in sexual organisms. Strict
66 uniparental inheritance does not allow for the generation of novel combinations of alleles
67 through recombination and has historically been expected to result in a buildup of deleterious
68 mutations, through a process known as Muller's ratchet (29, 30). However, the impact of
69 Muller's ratchet will depend upon the number of genes, which tends to be low in organelle
70 genomes (for example, there are 57 genes in Arabidopsis mitochondria (31)), and the rate of
71 deleterious mutation. In addition, there is accumulating evidence that biparental inheritance of
72 organellar genomes (sometimes referred to as paternal leakage) is more common than
73 previously appreciated (22, 23, 32, 33). Even infrequent biparental inheritance of organellar
74 DNA could represent a pathway for recombination, slowing or preventing the 'mutational
75 meltdown' associated with Muller's ratchet (34). Alternatively, recent theory posits that the
76 bottlenecking associated with uniparental inheritance of organellar genomes may actually
77 provide a benefit by increasing cell-to-cell variability and improving the efficiency of selection at
78 higher organizational levels (35-38). This benefit may explain why uniparental inheritance of
79 organellar genomes has been retained across eukaryotic lineages.

80 The number of genome copies per cell is another major difference between the nucleus
81 and organelles that impacts the spread of new mutations. In contrast to the single nuclear
82 genome copy that is passed to the next generation in each gamete, cells can contain numerous
83 mitochondria and plastids, and genome copies within each organelle can reach high numbers.
84 As such, a mutation arising in organellar DNA initially constitutes only a single member of a
85 larger population of non-mutant genome copies in the cell. The size of this population is
86 expected to influence the subsequent genetic dynamics. In Arabidopsis, only a few plastids are
87 present in meristematic cells, while over 50 plastids can be found in cells of mature leaves, and
88 the number of plastid genome copies per cell ranges from around 80 in meristematic tissue to
89 >3,000 in mature leaves (39). Mitochondrial genomes are present at ~50-100 copies in both egg
90 cells and leaf cells of Arabidopsis (40-42). However, in both cell types, the number of
91 mitochondria per cell exceeds 300 suggesting that many or most mitochondria do not contain a
92 full mitochondrial genome copy (41). The number of organellar genome copies in female
93 gametes of plants varies between species but is typically low, not exceeding 100 mitochondrial
94 genome copies (42). In comparison, a single mouse oocyte contains over 200,000 mitochondrial
95 genomes, the result of proliferation from ~200 mitochondrial DNA copies found in progenitor
96 germ cells of the embryo (8).

97 Mutation rates also differ among cellular compartments. In land plants, mitochondria
98 have the lowest mutation rate (as inferred from synonymous substitutions), followed by plastids

99 and then nuclei at a ratio of approximately 1:3:10 (24-26). By comparison, mammalian
100 mitochondrial sequence mutation rates greatly exceed those in the nucleus (26). Although plant
101 mitochondria and plastids have low rates of point mutation, their genomes undergo frequent
102 recombination between repeated sequences, resulting in populations of alternative structures
103 (43-45). Thus, reversible structural heteroplasmies can exist in plant mitochondria and have
104 been associated with cytoplasmic male sterility and other types of phenotypic variation (43, 46,
105 47).

106 Our previous work found that the nuclear-encoded protein MutS Homolog 1 (MSH1)
107 reduces plant organellar mutation rates (48), in addition to its previously characterized role in
108 suppression of ectopic recombination (49, 50). MSH1 is part of the larger MutS family of genes
109 involved in mismatch repair and has a unique architecture that includes both mismatch
110 recognition and endonuclease domains (51). It has been hypothesized that MSH1 initiates
111 double strand breaks (DSBs) at mismatched or damaged bases to facilitate repair through
112 homologous recombination (48, 52, 53). The high ploidies frequently associated with organelles
113 provide multiple genome copies for homologous recombination which plays a major role in DNA
114 replication and repair processes in plant organellar genomes (44, 54). Gene conversion is a
115 common outcome of DSBs and homologous recombination, resulting in homogenization of
116 genome copies within a cell (44, 54). It has been hypothesized that gene conversion could act
117 as an alternative mechanism to increase cell-to-cell variance in heteroplasmic frequencies in
118 eukaryotic lineages such as plants that may lack a physical bottleneck associated with germline
119 development (37). Thus, we predict the action of *MSH1* and other genes involved in
120 homologous recombination may accelerate the sorting of heteroplasmies.

121 We previously identified numerous mitochondrial and plastid heteroplasmies in
122 *Arabidopsis msh1* mutant lines and showed that some of these could be transmitted through
123 meristematic and reproductive tissues to subsequent generations (48). Having this unique
124 genetic material provided us the opportunity to study the dynamics of *de novo* heteroplasmies in
125 plants, both within individuals and across generations in *msh1* mutants and wild type
126 backgrounds. We find that heteroplasmic sorting is rapid in plants – particularly in plastids – and
127 that MSH1 function in mitochondria increases the speed of heteroplasmic sorting. For
128 heteroplasmic variants, we also found that GC base pairs preferentially increased in frequency
129 over AT base pairs. These results imply that gene conversion contributes to a high rate of
130 heteroplasmic sorting in plants and potentially biases the outcome of this sorting process.

131

132 **Results:**

133 **Identification of heteroplasmic variants in *msh1* mutants**

134 The *msh1* mutant background afforded us the opportunity to explore the dynamics of
 135 heteroplasmy in Arabidopsis. We selected ten high frequency single nucleotide variants (SNVs)
 136 resulting from de novo mutations that were identified in organellar DNA pools of *msh1* mutant
 137 plants (Table 1). Each SNV was associated with a specific *msh1* family line. All of the SNVs
 138 were transitions (GC→AT or AT→GC mutations), and the majority were in intergenic regions.
 139 The frequencies for each SNV measured by allele-specific droplet digital PCR (ddPCR) were
 140 repeatable and similar to those obtained from sequencing read counts (Table 1).

141 We used this ddPCR assay to identify heteroplasmy in individual plants by screening
 142 young leaves from the siblings and/or progeny of the plants used in the initial identification of
 143 SNVs (48). After adjusting for organellar genome copy number and numts (see Methods), only
 144 four of the ten SNVs were found to be heteroplasmic in any of the screened individuals; the
 145 other six variants had either reached fixation or were not detectable in the individuals screened
 146 (Table 1, Table S1). Therefore, we proceeded with these four heteroplasmic SNVs (two
 147 mitochondrial and two plastid) for all subsequent experiments and analyses. The number of
 148 heteroplasmic individuals identified was higher for the mitochondrial SNVs tested (46.5% of
 149 individuals) versus those from the plastid (3.7%) (Table S1), which is why a greater number of
 150 markers and total plants were screened for plastid versus mitochondrial SNVs.

Table 1. Characteristics of SNV targets.

SNV Target (nucleotide position)	Reference Nucleotide	Variant Nucleotide	Genetic Context	Variant Frequency (sequencing)*	Variant Frequency (ddPCR)*	Heteroplasmy Identified
Plastid (26553)	A	G	intergenic	0.076	0.0926 (0.0080)	Yes
Plastid (29562)	T	C	intergenic	0.032	0.026	No
Plastid (36873)	A	G	intergenic	0.059	0.032 (0.0024)	Yes
Plastid (48483)	A	G	intergenic	0.028	0.033	No
Plastid (61599)	A	G	intergenic	0.068	0.090	No
Plastid (72934)	A	G	<i>psbB</i> - CDS	0.023	0.017	No
Plastid (118559)	T	C	<i>ndhG</i> - CDS	0.014	0.015 (0.0082)	No
Mito (91017)	A	G	intergenic	0.147	0.180	Yes
Mito (143184)	T	C	<i>rrn26</i> - rRNA	0.014	0.012	No
Mito (334038)	C	T	intergenic	0.033	0.019 (0.0018)	Yes

*Variant frequencies are calculated as the count of variant alleles out of the total copy number in the sample. Variants were initially identified from Duplex Sequencing of purified organellar DNA from a pool of ~60 F3 plants (48). These same samples were used to estimate variant frequency with ddPCR. Standard deviation for ddPCR experiments is shown in parentheses for the SNVs used in subsequent studies, and seven to ten technical replicates were used for calculation of standard deviations.

151 ***Intergenerational heteroplasmic sorting occurs more rapidly in plastids than***
152 ***mitochondria in an msh1 mutant background***

153 To determine the frequency with which heteroplasmies are transmitted across
154 generations, we used *msh1* individuals that were each heteroplasmic for one of the four
155 identified SNVs as mothers to generate selfed progeny. We expected that variant frequencies in
156 the mother would influence the distribution of heteroplasmy in the progeny, so we used mothers
157 with a wide range of starting allele frequencies. Both mitochondria and plastid SNVs showed
158 rapid sorting over a single generation, as many progeny were fixed for either the wild type or
159 alternative (SNV) allele (Figure 1, Table S2). This trend was particularly striking in plastids: very
160 few heteroplasmic progeny were identified for plastid SNVs, regardless of the heteroplasmic
161 frequency in the mother. For mitochondrial SNVs, progeny showed a tighter and more
162 continuous distribution of heteroplasmy roughly distributed around the allele frequency of the
163 mother, with many progeny retaining a heteroplasmic state.

164 The distribution of heteroplasmy in progeny derived from a heteroplasmic mother can be
165 used to calculate an effective transmission bottleneck size (N). Although this measure has often
166 been (incorrectly) equated with the number of organellar genomes transmitted to the next
167 generation, it is more appropriately thought of as a relative metric to compare the cumulative
168 biological sampling variance in genome transmission throughout development and across
169 generations (14, 15). A common way of estimating bottleneck size is by taking the reciprocal
170 normalized sample variance, $\hat{N}_{sv} \simeq \bar{h} (1 - \bar{h})/s^2$, as an estimate for the number of effective
171 segregating units (14), where \bar{h} is the sample mean heteroplasmy and s^2 is the sample variance
172 in heteroplasmic frequencies for a set of tissue or progeny samples. However, the use of this
173 statistic is problematic for moderate samples of highly segregated cases, where the sample
174 variance approach yields estimates and uncertainties that are incompatible with the concept of
175 segregating units (for example, inferring $\hat{N}_{sv} < 1$ with confidence intervals that include zero) (55).
176 We took two approaches here to estimate bottleneck size. First, for comparison with previous
177 work, we used the above equation to calculate \hat{N}_{sv} , but we employed the population variance
178 (without Bessel's correction) for s^2 . This approach yields a slightly biased estimate but one that
179 respects heteroplasmy constraints ($\hat{N}_{sv} \geq 1$). More rigorously, we also used a maximum
180 likelihood approach based on the Kimura distribution (55) that captures these constraints in
181 order to identify the most likely value (\hat{N}) of the bottleneck parameter as well as the confidence
182 interval (CI) of this measure given a full set of observations. We also used this Kimura-based
183 approach to perform hypothesis testing (see Methods). Both values (\hat{N}_{sv} and \hat{N}) are reported in
184 tables for comparison, but we refer to the more rigorous Kimura estimates in the text.

185 Using data from seven plastid families and five mitochondrial families we found that,
186 over a single generation, plastids typically have a smaller transmission bottleneck size than
187 mitochondria (Table 2). Plastid transmission bottlenecks were extreme, approximating a value
188 of one ($\hat{N} = 1.06$, 95% CIs: 1.03-1.13), in accordance with observations that the vast majority of
189 offspring were homoplasmic for one allele or the other (Figure 1). The average mitochondrial
190 transmission bottleneck size in *msh1* mutants ($\hat{N} = 4.20$, 95% CIs: 4.15-4.25) was significantly
191 larger than in plastids ($p = 3.2 \times 10^{-55}$, likelihood ratio test, Table 2). Therefore, the number of
192 effective genome copies passed throughout development and from mother to progeny is larger
193 for mitochondria than for plastids. However, the transmission bottleneck values for both
194 organelles reflect relatively rapid heteroplasmic sorting.

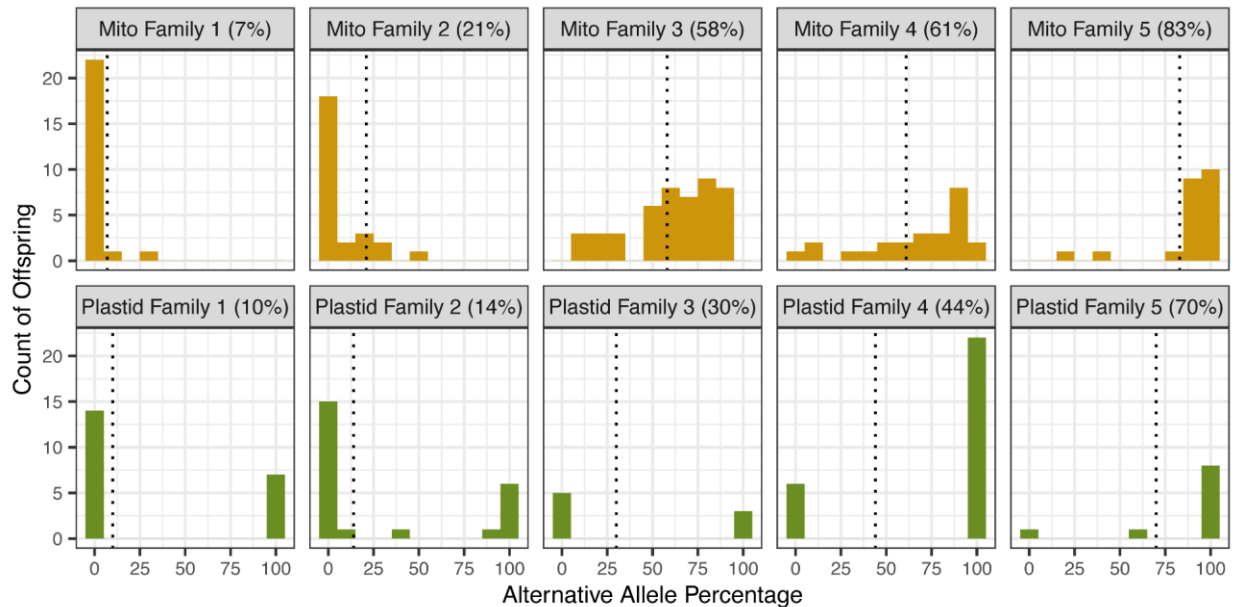


Figure 1. Distribution of heteroplasmy across generations in an *msh1* mutant background. Heteroplasmy (alternative allele frequency) was evaluated using ddPCR of leaf tissue in progeny of maternal lines with different levels of heteroplasmy, indicated by dotted vertical lines and numbers in parentheses on each graph. Histograms indicate the number of individuals showing different levels of heteroplasmy. Mitochondrial families (orange) are depicted in the top row, plastid families (green) are shown on the bottom row. For the sake of comparison with the five mitochondrial families, data for plastid families 6 and 7 in not shown but is included in Table 2.

Table 2. Effective transmission bottlenecks in organellar genomes in the *msh1* mutant background calculated for plastid and mitochondrial markers over single generations in *msh1* mutant plants. Confidence intervals for Kimura estimates are noted in parentheses below calculated bottleneck value. Likelihood ratio test (see methods) show that plastid bottlenecks are significantly smaller than mitochondrial bottlenecks ($p = 3.2 \times 10^{-55}$).

Family name	SNV target	Maternal sample % alternative allele	Progeny mean % alternative allele (\bar{h})	Number progeny (n)	Variance in heteroplasmy (s^2)	Bottleneck size estimate from s^2 (\hat{N}_{sv})	Bottleneck size estimate from Kimura fit (\hat{N} , 95% CIs)
Mito Family 1	Mito 91017	7	2	24	0.0052	3.54	2.81 (1.38-9.71)
Mito Family 2	Mito 334038	21	8	26	0.0186	3.79	3.18 (2.04-5.54)
Mito Family 3	Mito 91017	58	61	47	0.0573	4.14	4.68 (3.52-6.37)
Mito Family 4	Mito 91017	61	68	25	0.0822	2.65	3.33 (3.11-3.57)
Mito Family 5	Mito 91017	83	89	22	0.0356	2.69	6.14 (5.69-6.62)
						Mito mean 3.36	Joint mito 4.20 (4.15-4.25)
Plastid Family 1	Plastid 26553	10	33	21	0.2222	1.00	1 (1-1)
Plastid Family 2	Plastid 26553	14	31	24	0.1934	1.10	1.11 (1.03-1.35)
Plastid Family 3	Plastid 36873	30	38	8	0.2344	1.00	1 (1-1)
Plastid Family 4	Plastid 26553	44	79	28	0.1684	1.00	1 (1-1)
Plastid Family 5	Plastid 26553	70	86	10	0.0986	1.25	1.15 (1.02-2.25)
Plastid Family 6	Plastid 26553	7	16	20	0.1034	1.29	1.22 (1.06-1.76)
Plastid Family 7	Plastid 36873	7	0	20	0	NA	NA
						Plastid mean 1.07	Joint plastid 1.06 (1.03-1.13)

195 ***Heteroplasmic sorting in vegetative and floral tissues occurs more rapidly in plastids***
 196 ***than mitochondria in an msh1 mutant background***

197 Although reproductive tissue is one location where heteroplasmic sorting can happen, it
 198 can also occur within cells and tissues as they grow. This may be particularly important in
 199 organisms like plants that do not exhibit early germline specification (56, 57), a hypothesis that
 200 is supported by recent theory predicting ongoing segregation in plant tissues (37). We sampled
 201 multiple leaf and inflorescence tissues from selected progeny of *msh1* heteroplasmic mothers
 202 and quantified heteroplasmic rates (Figure 2, Table S3). Two plastid family lines (six individuals)
 203 initially selected for analysis showed no within-plant heteroplasmy and were either fixed for the
 204 wild-type or alternative SNV allele. The other family line showed high variance in heteroplasmy
 205 rates across tissues, indicative of rapid within-plant sorting. Using rates of heteroplasmy in the
 206 tissue samples from each plant, we found that within-plant bottleneck sizes were significantly

207 smaller on average for plastids ($\hat{N} = 5.92$, 95% CIs: 3.85-9.51) than for mitochondria ($\hat{N} = 12.00$,
208 CIs: 11.95-12.05, $p = 3.4 \times 10^{-29}$, likelihood ratio test; Table 3). Within-plant bottleneck size was
209 larger than the transmission bottleneck size seen between generations (plastids, $p = 2.4227 \times$
210 10^{-29} ; mitochondria, $p = 1.6 \times 10^{-30}$, likelihood ratio tests), suggesting that sorting during
211 vegetative growth indeed contributes to heteroplasmic variance, but the full reproductive cycle
212 and transmission to the next generation involves a tighter effective bottleneck.

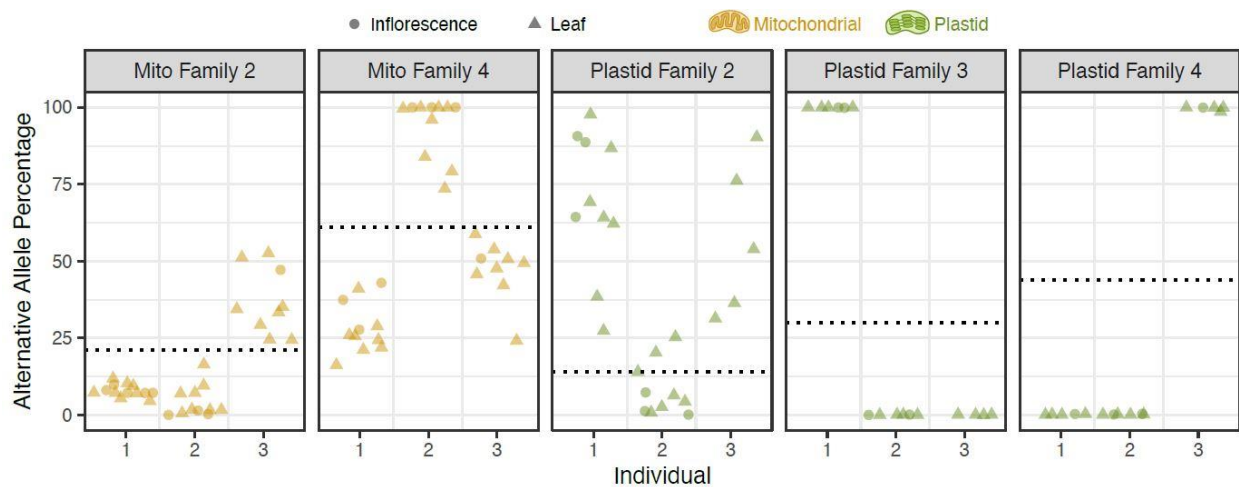


Figure 2. Distribution of heteroplasmy within individual plants in an *msh1* background. Progeny from mothers with varying levels of heteroplasmy (experiment shown in Figure 1) were selected for further analysis. Dotted lines indicate levels of maternal heteroplasmy. Levels of heteroplasmy (alternative allele percentage) for leaf and inflorescence tissues were determined using ddPCR.

Table 3. Within-plant bottlenecks in organellar genome transmission in *msh1* mutant backgrounds. Confidence intervals for Kimura estimates are noted in parentheses below calculated bottleneck value. Not applicable (NA) indicates that there was no variation within the tissues tested. Likelihood ratio test (see methods) show that within plant plastid bottlenecks are significantly smaller than mitochondria bottlenecks ($p = 3.4 \times 10^{-29}$).

Individual name	SNV target	Mean within-plant % alternative allele (\bar{h})	Number tissue samples (n)	Variance in heteroplasmy (s^2)	Within-plant Bottleneck size estimate from s^2 (\hat{N}_{sv})	Within-plant bottleneck size from Kimura fit (\hat{N} , 95% CIs)
Mt 3 - 2	Mito 334038	4	11	0.0024	16.87	18.82 (9.75-37.28)
Mt 3 - 1	Mito 334038	8	13	0.0004	192.46	195.83 (190.48-201.32)
Mt 9 - 1	Mito 91017	29	9	0.0105	22.19	23.06 (18.5-28.81)
Mt 3 - 3	Mito 334038	37	11	0.0066	30.88	32.28 (29.65-35.15)
Mt 9 - 3	Mito 91017	47	9	0.0085	29.27	28.17 (22.17-35.88)
Mt 9 - 2	Mito 91017	94	11	0.0090	6.37	4.17 (2.08-10.33)
					Mito mean 49.72	Joint mito 12.00 (11.95-12.05)
Pt 2a - 1	Plastid 26553	0	5	0	NA	NA
Pt 2a - 2	Plastid 26553	0	6	0	NA	NA
Pt 3 - 2	Plastid 36873	0	6	0	NA	NA
Pt 3 - 3	Plastid 36873	0	4	0	NA	NA
Pt 2b - 2	Plastid 26553	8	10	0.0069	10.91	12.48 (6.75-23.94)
Pt 2b - 3	Plastid 26553	58	5	0.0513	4.76	5.18 (2.28-14.65)
Pt 2b - 1	Plastid 26553	69	10	0.0475	4.50	5.22 (2.93-10.22)
Pt 2a - 3	Plastid 26553	100	5	0	NA	NA
Pt 3 - 1	Plastid 36873	100	6	0	NA	NA
					Plastid mean 6.72	Joint plastid 5.92 (3.85-9.51)

213 ***MSH1* activity accelerates heteroplasmic sorting in mitochondria**

214 Because *MSH1* is hypothesized to introduce DSBs and promote recombinational repair (48, 52,
 215 53), we predicted that a functional copy of the *MSH1* gene would speed up heteroplasmic
 216 sorting by homogenizing genome copies through gene conversion, as predicted by theoretical
 217 modeling (37). To test this hypothesis, we transferred heteroplasmic variants to a wild-type
 218 background by crossing heteroplasmic *msh1* female plants with wild-type males and analyzing
 219 heteroplasmy levels in both F1 and F2 (selfed) progeny. All plants were genotyped at the *MSH1*
 220 locus, and only individuals that were heterozygous or homozygous wild type were included in

221 the heteroplasmy analysis (the *msh1* mutation is recessive). Due to the extremely low number
222 of individuals that were heteroplasmic for plastid SNVs and the rapid plastid heteroplasmic
223 sorting rates, this backcrossing method was only successful in generating lines to study
224 mitochondrial heteroplasmy. For mitochondrial SNVs in the wild-type background, we saw
225 extremely rapid sorting of heteroplasmies (Figure 3, Table S2, Table S4), akin to our
226 observations in plastids under *msh1* mutant backgrounds (Figure 1). The average mitochondrial
227 transmission bottleneck size for wild-type plants ($\hat{N} = 1.33$, 95% CIs: 1.20-1.54) was significantly
228 reduced from that in the *msh1* mutant background ($\hat{N} = 4.20$, 95% CIs: 4.15-4.25, $p = 8.1 \times 10^{-49}$,
229 likelihood ratio test; Table 2, Table 4). The standing number of organellar genomes per
230 nuclear genome copy in leaf tissue did not differ significantly between *msh1* and wild type
231 backgrounds (Figure S1), suggesting that the differences we identified in heteroplasmic sorting
232 were more likely due to differences in MSH1 activity rather than changes in the physical number
233 of organellar DNA copies per cell.

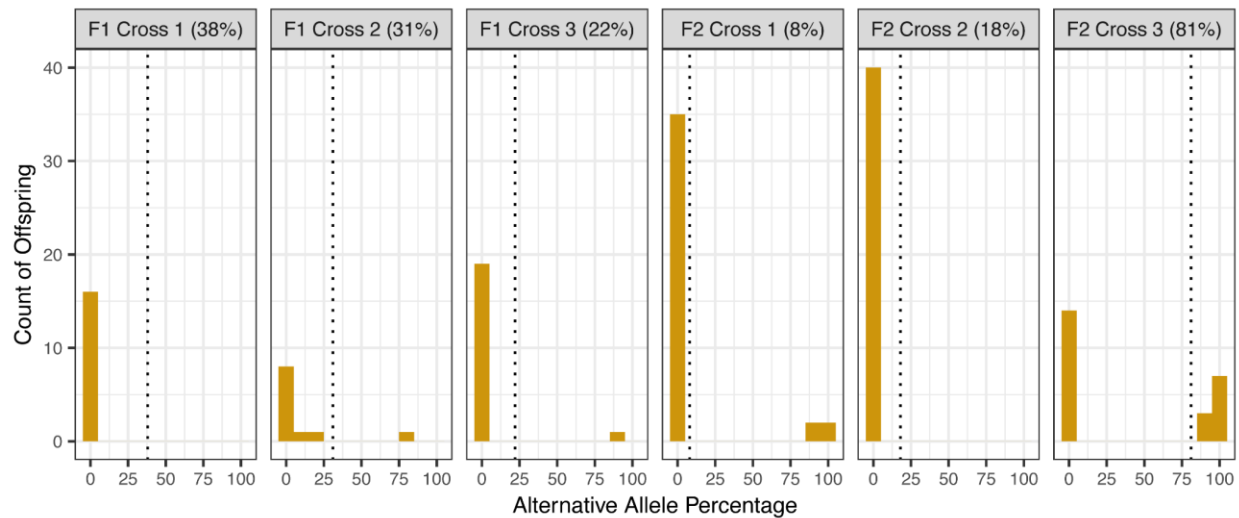


Figure 3. Distribution of mitochondrial heteroplasmy across generations in a wild-type background. Mitochondrial heteroplasmies were backcrossed into a wild-type *MSH1* background. Heteroplasmy (alternative allele frequency) was evaluated using ddPCR of leaf tissue in progeny of maternal lines with different levels of heteroplasmy, indicated by vertical dotted lines and numbers in parentheses on each graph. Histograms indicate the number of individuals showing different levels of heteroplasmy. All three F2 mothers were progeny from F1 Cross 2.

Table 4. Effective transmission bottlenecks in organellar genomes in wild type background. Effective transmission bottleneck size was calculated for mitochondrial markers over single generations in wild type plants. Confidence intervals for Kimura estimates are noted in parentheses below calculated bottleneck value. Not applicable (NA) indicates that there was no variation within the progeny – they were all fixed for one allele or the other. Note that bottleneck size estimates for F1 cross 1 are imprecise because they are based on a family in which only one of 17 progeny remained heteroplasmic and that individual had a low allele frequency (2%). The large point estimates for that family weigh heavily when taking a mean of \hat{N}_{sv} estimates but do not bias the joint maximum-likelihood estimate of \hat{N} .

Cross type	SNV target	Maternal sample % alternative allele	Progeny mean % alternative allele (\bar{h})	Number progeny (n)	Variance in heteroplasmy (s^2)	Bottleneck size estimate from s^2 (\hat{N}_{sv})	Bottleneck size estimate from Kimura fit (\hat{N} , 95% CIs)
F1 cross 1	Mito 334038	38	0.14	17	0.00003	46.13	18.18 (2.45-204.07)
F1 cross 2	Mito 334038	31	8	10	0.05867	1.63	1.94 (1.26-4.45)
F1 cross 3	Mito 91017	22	5	20	0.03708	1.15	1.58 (1.13-3.67)
F2 cross 1	Mito 334038	8	18	32	0.13963	1.05	1.26 (1.11-1.62)
F2 cross 2	Mito 334038	18	0	37	0.00000	NA	NA
F2 cross 3	Mito 334038	81	36	24	0.21511	1.07	1.24 (1.11-1.54)
						Mean 10.21	Joint estimate 1.33 (1.20-1.54)

234 **GC-biased inheritance in organellar genomes**

235 The fact that the SNVs used in our analysis were GC→AT or AT→GC transitions
 236 created the opportunity to search for GC or AT bias in the inheritance of SNVs in plant
 237 organellar genomes. Using the allele frequency data from our heteroplasmic mothers and
 238 progeny, we found that, even though angiosperm organelle genomes are typically AT rich (58),
 239 there is evidence of a GC bias during heteroplasmic sorting in both plastids and mitochondria
 240 (Figure 4, Table S5). The frequency of the GC allele increased in the progeny relative to the
 241 mother in 14 of 17 families (two-sided binomial test, $p = 0.0127$). Although modest increases in
 242 the frequency of the GC allele were found in most lines, five showed that mean progeny GC
 243 frequency increased over 20% compared to the mother (Figure 4B). The mean increase in
 244 frequency for the GC allele was 14.1%, which differed significantly from zero (two-sided t-test, p
 245 = 0.0039). The magnitude of this increase was nearly identical for mitochondrial SNVs (14.0%)
 246 and plastid SNVs (14.2%).

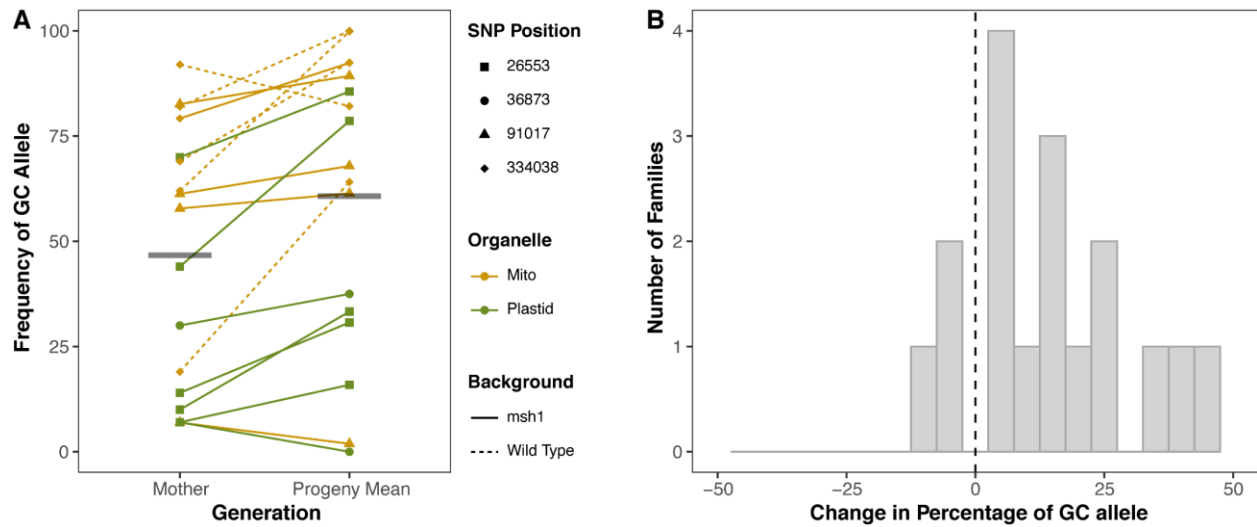


Figure 4. Changes in frequency of GC alleles between generations. A) Norm of reaction plot showing the frequency of GC alleles (the SNVs from this study) in mothers and progeny (mean value). The reference (wild type) allele was AT and the variant GC in all cases except for mt334038 in which the inverse was true (Table 1). Means for each group are shown with horizontal gray bars. B) Histogram showing the change in percentage of GC alleles for tested family lines. A two-sided t-test shows bias toward GC alleles, $p = 0.0039$.

247 **Discussion:**

248 ***Potential causes of rapid heteroplasmic sorting in plant organelles***

249 In *Arabidopsis*, we found that both plastid and mitochondrial heteroplasmies sorted out
 250 to homoplasmy within one to a few generations and exhibited tight effective bottlenecks,
 251 regardless of whether they were found in wild type or *msh1* mutant backgrounds (*msh1* plastid
 252 $\hat{N} \approx 1$, *msh1* mitochondria $\hat{N} \approx 4$, wild-type mitochondria $\hat{N} \approx 1.3$). In contrast, effective
 253 mitochondrial germline bottlenecks are estimated to be substantially larger in most animal
 254 systems: ~ 5 -10 in *Daphnia* (59), ~ 9 in macaques (60), ~ 10 -30 in humans (16-19), ~ 30 in
 255 *Drosophila* (61), ~ 60 in *Caenorhabditis elegans* (62), ~ 80 in salmon (63), 5-100 in mice (9, 55),
 256 and 170 in zebrafish (64). Thus, in animals, heteroplasmy is often retained over multiple
 257 generations.

258 Germline bottlenecks are well established as drivers of heteroplasmic variance in
 259 animals, but the mechanism is still not completely understood (8, 9, 14, 18). The bottleneck is
 260 thought to be due, at least in part, to the physical reduction of mitochondrial DNA copies during
 261 female germline development (65, 66). However, other lines of evidence suggest that selection
 262 (67-69), mitochondrial dynamics (12), and preferential genome amplification (11, 13) can also
 263 play roles in reducing the effective population size of mitochondrial genomes.

264 In plants, where the germline is segregated later in development (56, 57, 70), the way in
265 which heteroplasmic variance increases is even less clear. However, the relatively modest
266 number of mitochondrial and plastid genome copies in meristematic and reproductive tissues is
267 a likely contributor to rapid heteroplasmic sorting. In plants, all aboveground tissues, including
268 reproductive organs, are derived from the shoot apical meristem (SAM). Arabidopsis SAM cells
269 contain only ~80 copies of plastid DNA housed within 4-10 proplastids (39). The number of
270 mitochondrial genome copies in SAM cells is not well established, but these values are typically
271 <100 in both vegetative tissues and egg cells (40-42). Additional mechanisms, including
272 selection could reduce the effective population size of organelle genomes by acting as an
273 effective germline bottleneck. The frequent recombination associated with plant organellar
274 genomes (44, 54) could also act as an effective bottleneck by homogenizing genomes through
275 gene conversion without requiring a physical reduction in organelle DNA copy number, as
276 predicted by recent theory (37). The rapid heteroplasmic sorting in Arabidopsis organelles, as
277 well as our finding that MSH1 activity further accelerates the rate of sorting (see below),
278 supports this hypothesis.

279 Although the rate of heteroplasmic sorting has not been studied extensively in plants,
280 there are supporting lines of evidence that this process may be rapid in other angiosperms. For
281 example, controlled crosses of *Silene vulgaris* and *Daucus carota* have shown that
282 mitochondrial heteroplasmy is maternally transmitted at only low levels across generations (20,
283 21). Mitochondrial variants produced by repeat-mediated recombination have been observed to
284 rapidly rise from mean cellular copy numbers under one to high frequencies or even
285 homoplasmy across cells, through a process called substoichiometric shifting (SSS) (43, 46).
286 Because of the role of *MSH1* in recombination surveillance, these structural variants arise more
287 frequently in *msh1* mutants (50), but the causes of rapid SSS have remained less clear. Studies
288 of variegation mutants derived from biparental plastid inheritance show that sorting occurs
289 rapidly at the level of whole organelles and is frequently complete within a single generation (15,
290 28, 71). When plastid DNA is modified using a transgenic approach, homoplasmy is typically
291 reached after a few rounds of antibiotic selection (72, 73). The rapid sorting of transgenic plastid
292 mutations has also been observed in the absence of antibiotics (74). It is currently unclear
293 whether rapid sorting of plastid transgenes occurs in all plants as it has been extremely difficult
294 to obtain homoplasmic transgenic lines of various species, particularly monocots (75-77).
295 However, this may be due to the general recalcitrance of these species to plastid transformation
296 or inefficient selection that makes variants difficult to detect (75, 76). The approach we have
297 used here would be valuable to test heteroplasmic sorting in other species because most

298 intergenic SNVs are unlikely to be under strong selective pressure, as opposed to the entire
299 genes that are introduced with transgenic approaches or the large structural rearrangements
300 associated with SSS. The rapid sorting we have identified could readily explain these diverse
301 instances of segregation and occasional amplification of rare variants in organellar genomes,
302 but characterization from diverse species is needed because the developmental and genetic
303 mechanisms of heteroplasmic sorting may vary across plant lineages. However, the elevated
304 germline expression of recombination machinery including MSH1 appears to be conserved
305 across several angiosperms (37), suggesting a similar genetic basis may exist for generating
306 heteroplasmic variance.

307

308 ***Differences in heteroplasmic sorting between mitochondria and plastids***

309 In the *msh1* mutant background, we found that plastids had tighter bottlenecks than
310 mitochondria, both across generations ($\hat{N} = \sim 1$ versus ~ 4 , respectively) and within individuals (\hat{N}
311 $= \sim 6$ versus ~ 12 , respectively). This result may seem surprising because the much greater
312 relative copy number of plastid versus mitochondrial DNA typically seen in most aboveground
313 tissues (39, 41) would be expected to result in lower levels of heteroplasmic variance in plastids
314 (i.e., a wider bottleneck size). However, as noted above, mitochondria and plastids both
315 possess low genome copy numbers in the SAM and/or reproductive tissues (39-42), presenting
316 similar potential for physical bottlenecks. One key difference between the two types of
317 organelles is that mitochondria can experience both full and transient fusion events over the
318 plant life cycle allowing for genetic exchange, whereas plastids rarely if ever fuse (15, 78-82).
319 Mitochondrial fusion is particularly prevalent in the SAM, where it is estimated that 80% of the
320 mitochondrial volume is fused into a dynamic tentaculate cage-like structure, creating the
321 opportunity for sharing of genome copies between formerly distinct mitochondrial compartments
322 (79). Here, gene conversion is predicted to homogenize the mitochondrial genomes within a cell
323 leading to increased heteroplasmic variance between cells (37, 79, 83). Thus, all else being
324 equal, existing theory would predict that fusion results in more rapid heteroplasmic sorting in
325 mitochondria than plastids – the opposite of what we observed. This suggests that other
326 differences in organelle biology can impact the rate of variability in organellar DNA populations.

327 Additional factors are expected to influence the speed of heteroplasmic sorting, but the
328 extent to which they differ between plastids and mitochondria is often unclear. These processes
329 include the number of organelles per cell, rates of organellar DNA replication and degradation,
330 rates of organelle turnover, the physical partitioning of organellar DNA during organelle
331 replication, and the partitioning of whole organelles during cell division (15). In addition, plastids

332 and mitochondria house distinct versions of many DNA replication, recombination and repair
333 proteins (54), which could influence relative rates of gene conversion. It is also possible that
334 dual-targeted proteins involved in these pathways, such as MSH1, may differentially impact
335 gene conversion rates between organelles. All of these factors likely vary based on cell type and
336 developmental stage, and they may work in combination. Models of heteroplasmic sorting have
337 tried to integrate many of these factors, but much of the relevant biological data required for
338 parameterization is still lacking, particularly in plant systems (9, 14, 18, 37, 84).

339

340 ***The role of MSH1 in heteroplasmic sorting***

341 We found that mitochondrial heteroplasmic sorting was faster in wild type Arabidopsis
342 plants than in *msh1* mutants ($\hat{N} = \sim 1.3$ versus ~ 4 respectively), with the majority of wild type
343 progeny reaching fixation for either the reference or alternative allele within a single generation.
344 This result lends support to the hypothesized repair mechanism in which MSH1 identifies
345 mismatches and initiates DSBs followed by template-based recombinational repair [(48, 52, 53),
346 Figure 5A]. Under this model, MSH1 would increase rates of gene conversion, thereby
347 homogenizing genome copies within cells and increasing variance among cells [(37), Figure
348 5B]. Somewhat confusingly, MSH1 is primarily known as a recombination suppressor because it
349 performs organellar genome surveillance, preventing *illegitimate* recombination between small
350 repeats that can result in genome rearrangements and instability (49, 50). However, this role is
351 not contradictory to the hypothesis that MSH1 activity increases the overall rate of *homologous*
352 recombination. Indeed, these patterns may well reflect the same mechanism of action, in which
353 MSH1 promotes homologous recombination by introducing DSBs at any mismatched bases,
354 regardless of whether they were generated by strand invasion between short/imperfect repeats
355 or by DNA replication errors. Although we might predict that this same mechanism would
356 increase heteroplasmic sorting rates in plastids, we were unable to generate wild type plants
357 that were heteroplasmic for plastid markers – thus the role of MSH1 in plastid heteroplasmic
358 sorting remains an open question.

359 Another way in which MSH1 could alter sorting dynamics is through changing the
360 physical interactions and fusion events between mitochondria. Hypocotyl cells of *msh1* mutants
361 show increased mitochondrial connectivity over wild type (85), suggesting an increased capacity
362 for genome mixing and homogenization. Under existing models (14, 37), increased rates of
363 fusion are predicted to accelerate mitochondrial sorting, the opposite of what we see in *msh1*
364 mutants. However, if the lack of functional MSH1 results in lower rates of gene conversion,
365 higher rates of mitochondrial fusion may not be sufficient to increase cell to cell variance. This

366 observation, in combination with the finding that plastids sort faster than mitochondria even
 367 though they do not undergo fusion, suggests that the relationship between fusion and
 368 heteroplasmic sorting may be more complex than suggested by current models.

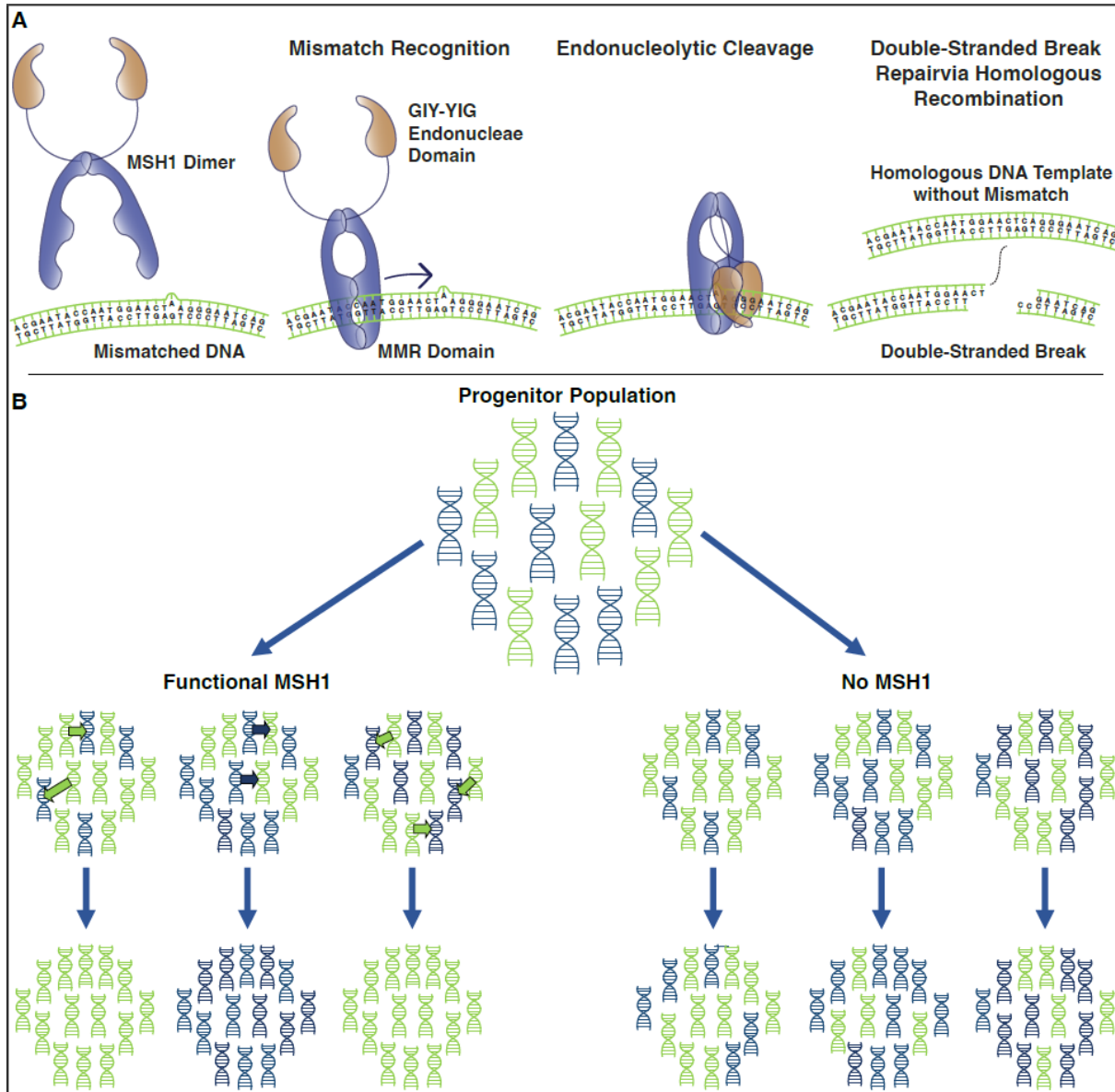


Figure 5. Hypothesized model for role of MSH1 in accelerating heteroplasmic sorting. A) Previously hypothesized mechanism (48, 52, 53) through which MSH1 promotes homologous recombination and repair. The mismatch repair (MMR) domain of dimeric MSH1 slides along organellar DNA until it reaches a mismatch, inducing a conformational change in the protein such that the GIY-YIG endonuclease domain creates a double strand break in the DNA. This break is then repaired via homologous recombination (gene conversion). B) Hypothesized process (37) through which MSH1-induced gene conversion increases rate of heteroplasmic sorting in mitochondria. A heteroplasmic progenitor population contains two different alleles (green and blue). When MSH1 is present (left), it promotes gene conversion events (arrows), resulting in faster homogenization of gene copies within populations and increased variance among populations. In the absence of MSH1 (right) these gene conversion events are less common and variation in heteroplasmic frequencies accumulates more slowly.

369 **Evidence for GC-biased gene conversion in plant organelles**

370 Organellar genomes, including those of Arabidopsis (31, 86), are typically AT rich but
371 also exhibit a wide range in nucleotide composition (58). The reasons for these biases are not
372 fully understood, but most organisms across the tree of life experience an AT-biased mutation
373 spectrum (87-89). However, in nuclear genomes, this mutation bias may be offset to varying
374 extents by GC-biased gene conversion (90, 91). The possibility for biased gene conversion in
375 plant organellar genomes is largely unexplored, and the few studies that have investigated this
376 in plastids have come to differing conclusions about GC versus AT bias (92-94). In the SNVs
377 studied here, we found evidence for GC-biased changes in allele frequency in both plastids and
378 mitochondria, as well as in *msh1* and wild-type backgrounds. Notably, we observed this bias
379 regardless of whether the mutant allele was AT (Mito 334038) or GC (Mito 91017, Plastid
380 26553, and Plastid 36873). Thus, it appears to be directly related to nucleotide composition and
381 not a systematic preference for or against the reference allele. All four SNVs that were tracked
382 in this study were in intergenic regions (Table 1), reducing the likelihood that the variants alter
383 organellar or cellular function. In human mitochondria, variants in the non-coding D-loop did not
384 show significant selection against pathogenic alleles; however, a broad population study
385 showed a notable absence of variants in sites involved in gene transcription and mitochondrial
386 DNA replication, in addition to other non-coding sites with no known function (10). Thus, a bias
387 due to selection on functional effects of the variants studied here cannot be ruled out, especially
388 given the incomplete characterization of regulatory elements and non-coding RNAs in plant
389 organelle genomes (95-98).

390 If the observed GC bias is driven by gene conversion, it would suggest that the GC allele
391 is favored during homologous recombination between heterogeneous DNA copies. In
392 mitochondria, gene conversion could happen within heterogeneous organelles, but we expect it
393 to be a particularly powerful actor during fusion in the SAM. In plastids, which do not undergo
394 fusion, gene conversion is only expected to take place within organelles (not between
395 organelles). This raises an important point about our sampling design. The SNVs we tracked
396 are inferred to have arisen in the F2 generation, but we sampled mothers from later generations
397 (F3 to F5 in plastids, Table S1). Therefore, we did not analyze the initial dynamics of plastid
398 variants at their inception when they were present at low frequency among the genome copies
399 within a single plastid. It is possible that some or even all of the plastids in our sampled mothers
400 had already reached homogeneity for one allele or another, meaning that heteroplasmy
401 dynamics were playing out among rather than within plastids. However, if the observed trend
402 towards increasing frequency of GC alleles is the result of gene conversion bias, it would

403 suggest that the mother plants in our study still contained plastids with copies of both alleles.
404 This may be the case, but our data suggest extremely rapid heteroplasmic sorting, which might
405 be expected if it were happening at the level of the small number of whole plastids within a cell.
406 On the other hand, if the sets of genomes within each plastid had already reached homogeneity,
407 it would suggest some unknown mechanism favoring GC alleles. These uncertainties
408 emphasize the importance of determining how the rate of sorting among the genome copies
409 within a plastid compares to the sorting process among the multiple plastids within a cell.

410

411 **Conclusions**

412 The mechanisms of organellar genome maintenance and transmission are
413 fundamentally different in plants and animals, but very little is known about how this affects the
414 fate of variants arising from de novo mutations. We found that heteroplasmies in Arabidopsis
415 organelles sort very rapidly which is likely due to a combination of low genome copy numbers in
416 germline/progenitor cells and the recombinational nature of plant genomes. Our work supports a
417 role for gene conversion as an important mechanism facilitating rapid sorting of heteroplasmic
418 variants in Arabidopsis, which has been hypothesized to be a key mechanism for increasing
419 variance in eukaryotic systems without early germline sequestration (37). Notably, the
420 recombination surveillance and DNA repair gene *MSH1*, which is absent from most eukaryotic
421 systems including animals (48), may play a key role in this process.

422

423

424 **Methods:**

425 ***Plant material***

426 Two homozygous *msh1* (At3g24320) mutant lines containing point mutations that result
427 in either a nonsense mutation (CS3372: *chm1-1*) or an aberrant splice site (CS3246: *chm1-2*)
428 were obtained from the Arabidopsis Biological Resource Center (50). Crossing design and
429 techniques used for identification of de novo mutations are described previously (48). Briefly,
430 homozygous mutants were used as males in crosses onto wild-type plants. The resultant F1
431 plants were allowed to self-pollinate, seed was planted and homozygous *msh1* lines (F2
432 families) were identified. The F2 lines were allowed to self-pollinate, and mitochondria and
433 chloroplast were isolated from their progeny (pools of F3 plants). Organellar DNA was extracted
434 and analyzed with Duplex Sequencing (99) to identify de novo mutations. High frequency SNVs
435 identified in F3 organellar DNA pools from *msh1* lines were used in this study (Table 1).

436 In initial experiments, seeds were vernalized in water for 3 days at 4 °C, planted directly
437 into 3-inch pots containing Pro-Mix BX media and grown on light shelves under short day
438 conditions. Heteroplasmic individuals were moved to long (16 h light) day conditions when they
439 began to bolt. Once siliques were ripe, all seeds were harvested in bulk. Seeds of heteroplasmic
440 mothers from lines selected for further analysis were sterilized and plated on MS-agar (100),
441 vernalized for 3 days at 4 °C and placed on light shelves to germinate. When seedlings had two
442 true leaves, they were transferred to 1-inch pots filled with Pro-Mix BX media and placed in a
443 growth chamber under short (10 h light) day conditions. Plants were transferred to long day
444 conditions upon bolting.

445

446 ***DNA extraction and heteroplasmy analysis***

447 Tissue samples were disrupted using the TissueLyser (Qiagen), and total cellular DNA
448 was extracted using the Qiagen Plant DNeasy kit. In cases where tissue was limiting (e.g.,
449 inflorescences), DNA was extracted by grinding tissue in 200 mM Tris-HCl pH 9.0, 250 mM
450 NaCl, 25 mM EDTA, and 1% SDS, followed by precipitation in isopropanol. gDNA was
451 quantified using Qubit (concentrations ranged from 0.5 - 30 ng/μL), and gDNA integrity of
452 selected samples was checked by agarose gel electrophoresis.

453 Heteroplasmy analysis was performed with allele-specific ddPCR assays essentially as
454 described in Wu et al. 2020 (48). Primers and probes for ddPCR were designed to ten different
455 high-frequency SNV targets, seven in the plastid and three in the mitochondria (Table 1).
456 Primers (Table S6) were designed to amplify fragments of 130 – 250 bp, with the SNV in the
457 middle of the amplified sequence. Probes (Table S7) were designed to either the reference
458 sequence or the variant sequence with the target SNV in the center. All primers and probes
459 were synthesized by Integrative DNA Technologies.

460 ddPCR reactions were composed of: Bio-Rad ddPCR Super Mix for Probes (no dUTP),
461 250 nM final concentration of each (reference and variant) probe, 900 nM final concentration of
462 each primer (F and R), 1 μL of the restriction enzyme BglIII (which is used to fragment template
463 DNA but is not predicted to cut within any of the amplified products), and 5 μL of an appropriate
464 dilution of DNA in a 20 μL total reaction. Droplet generation was performed using a Bio-Rad
465 QX200 Droplet Generator as per the manufacturer's instructions, and PCR was performed in a
466 Bio-Rad C1000 with a deep-well block under the following thermal cycling conditions: enzyme
467 activation at 95 °C for 10 min, 40 cycles of 94 °C for 30 sec, annealing/extension temperature
468 (see Table S6) for 1 min, and deactivation of the polymerase and restriction enzyme at 98 °C for

469 10 min – with a ramp speed of 2 °C per sec for all steps. Droplets were read on the Bio-Rad
470 QX200 Droplet Reader and analyzed using QuantaSoft Analysis Software (Bio-Rad).

471 Dilutions of mutant (*msh1*) organellar DNA (48) were used to verify the presence of the
472 SNV in the original mutant F3 organellar extractions alongside paired wild type samples to
473 check for probe specificity. Wild type and mutant organellar samples and no template controls
474 were used to determine appropriate annealing temperatures for each primer probe set to
475 minimize off target binding in wild type and increase separation of positive and negative droplets
476 in both channels. Positive and negative controls were always run alongside experimental
477 samples to ensure assay fidelity and verify appropriate settings for channel thresholds.
478 Background rates of the variant probe binding to wild type samples were typically very low <
479 0.05%. Experimental samples with variant calls falling at or under wild type values were set to
480 zero for further analyses.

481

482 ***Organellar genome copy number***

483 Evagreen ddPCR was performed, essentially as described previously (101) to determine
484 the number of mitochondrial and plastid genomes per nuclear genome copy. The reason for this
485 was two-fold. First, it was important to determine whether the *msh1* mutant background altered
486 the relative numbers of organellar genome copies. Secondly, numts (nuclear mitochondrial
487 DNA, i.e., copies of mitochondrial DNA inserted into the nuclear genome) are known to be
488 present in the *A. thaliana* nuclear genome (102-104) and we wanted to correct for this in our
489 heteroplasmy analysis.

490 Two primer sets were used per genome to determine copy number (Table S1). Nuclear
491 genome markers were single copy and located on chromosomes 1 and 2. Organellar markers
492 were designed to single-copy mitochondrial (*rps12* and *cox2*) and plastid (*clpP1* and *psaA*)
493 genes. For the nuclear genome, values from each primer set were averaged and used to
494 calculate the number of organellar genome copies per nuclear genome for each organellar
495 primer set. For plastids, values from each primer set were averaged to generate a final number
496 of plastid copies per nuclear genome. For mitochondria, both primer sets amplify numts, so the
497 values were adjusted based on the number of numt copies. The amplified regions of *cox2* and
498 *rps12* are present at one and three numt copies, respectively, in the Arabidopsis nuclear
499 genome (104). These values were subtracted from the calculated values of mitochondrial copies
500 per genome before averaging to obtain a final value. Our mitochondrial SNVs of interest
501 (mt91017 and mt334038) are both present in three copies in the Arabidopsis nuclear genome
502 (104).

503 The number of organellar genomes per nuclear genome were determined for paired wild
504 type and *msh1* mutants that were grown in parallel. Leaves were sampled when plants were 8
505 weeks old. For tissue specific analyses of mitochondrial genomes, samples consisted of whole
506 inflorescences (n = 13) and 8-week-old leaf tissue: old leaves harvested from the base of the
507 rosette (n = 12), and young leaves harvested from the top of the rosette (n = 16). A smaller
508 subset of these was used to determine tissue specific amounts of plastid genomes. For each
509 tissue, an average value was calculated for mitochondrial and plastid genomes per nuclear
510 genome.

511 We used experimentally determined values of organellar genome copy number along
512 with the deduced number of numt copies for each mitochondrial SNV ($Nu = 3$ in both instances)
513 to correct our heteroplasmy values by computing a correction factor as described below:

514

515 Correction factor for numts in heteroplasmy data, $M = (O + Nu) / O$

516

517 Where O = organellar genomes per nuclear genome copy, and Nu = nuclear genome copies of
518 the SNV. The alternative allele frequency for a sample was multiplied by the correction factor M .

519

520 ***Heteroplasmy sampling across generations***

521 To understand the extent to which heteroplasmy is transmitted across generations, we
522 identified heteroplasmic individuals in an initial screen and then analyzed the distribution of
523 allele frequencies in their progeny using ddPCR. Initial screens to identify heteroplasmic
524 mothers were conducted on F3 and/or F4 *msh1* mutant individuals. Leaves were sampled after
525 4-6 weeks of growth. Seeds from heteroplasmic individuals were sown and an initial leaf sample
526 was taken from each offspring after 4 weeks of growth.

527

528 ***Heteroplasmy sampling within plants***

529 To understand how heteroplasmy is distributed within individuals, we selected three
530 plants from each heteroplasmic mother (described above) for further tissue sampling. Three
531 fully expanded rosette leaves were harvested from each plant at 5 weeks of growth. At 8 weeks
532 of growth, leaves from the top (young) and base of the rosette (old) were harvested. Once
533 plants began to bolt, entire single inflorescences were harvested. Selected tissue samples (8-
534 week-old leaves and inflorescences) from this experiment were used to determine organellar
535 genome copy number in experiments described above. This initial experiment did not lead to the

536 identification of individuals heteroplasmic for plastid markers, so additional plastid SNV lines
537 were grown and tissues were sampled in a subsequent experiment of the same design.

538

539 ***Bottleneck calculations***

540 We used two methods for estimating bottleneck size. First, we applied the common approach
541 based on measures of heteroplasmic variance:

542

$$543 \quad \hat{N}_{sv} = \bar{h} (1 - \bar{h}) / s^2$$

544

545 where s^2 is the variance of heteroplasmic frequency in progeny (or within a plant), $(1/n) \sum (h_i -$
546 $\bar{h})^2$, and \bar{h} and h_i are the sample mean and individual heteroplasmic frequencies of offspring (or
547 tissues), respectively. In our intergenerational analysis, we used the offspring mean as an
548 approximation of the maternal heteroplasmic frequency, even though we obtained experimental
549 estimates of maternal heteroplasmy levels. This approach was chosen because we saw bias
550 towards GC alleles (Figure 4), suggesting that maternal values would not be an effective
551 estimate of average offspring values.

552 The second approach we took to estimate the bottleneck size was using a Kimura model
553 (55). Here we maximized the joint likelihood of a set of heteroplasmy measurements under the
554 Kimura model, which takes two parameters: mean heteroplasmy (p) and bottleneck parameter
555 b . b is related to the effective "bottleneck size" N by $N = 1/(1-b)$. Previous work has proposed
556 simply setting the population parameters to match the sample statistics p and b (55), but as this
557 does not in general yield the maximum likelihood parameter estimates, it can give misleading
558 results and does not support hypothesis testing. Instead, we used the kimura package in R
559 (<https://github.com/lbozhilova/kimura>) to compute likelihoods and optimization using Nelder-
560 Mead and Brent algorithms (105) to explicitly find the maximum likelihood parameters and the
561 Fisher information matrix, from which we derive 95% confidence intervals. For homoplasmic
562 cases, numerical issues challenged the Fisher approach, and bootstrap resampling with 200
563 resamples was instead used to estimate confidence intervals.

564 For hypothesis testing regarding the bottleneck size in two different groups of sample
565 sets, we considered two statistical models. First, each set of samples is generated from the
566 Kimura distribution with a set-specific p and a group-specific b . Second, each set of samples is
567 generated with a set-specific p and a b common to both groups. For example, consider a
568 comparison between mitochondrial and plastid intergenerational bottlenecks. In the first model,
569 each family would have its own p , mitochondrial families would have one b value, and plastid

570 families would have another b value. In the second model, each family would have its own p
571 and a b common to all families. We then maximize the joint likelihood over all observations for
572 the two models and conduct a likelihood ratio test with one degree of freedom, reflecting the
573 additional b parameter in the first model. When reporting bottleneck size across samples in a
574 given group (for example, across *msh1* mitochondrial families), we give the maximum likelihood
575 estimate (\hat{N}) and confidence intervals from this within-group inference. All code is freely
576 available at <https://github.com/StochasticBiology/plant-odna-sorting/>.

577

578 ***Impact of MSH1 on heteroplasmy transmission***

579 To determine whether MSH1 influences the spread of heteroplasmy across generations,
580 we backcrossed *msh1/msh1* mutant females heteroplasmic for an SNV (either mt334038 or
581 pt26553) to wild-type males. A minimum of 20 F1 plants were tested for heteroplasmy.
582 Heteroplasmic plants were self-pollinated, and then F2 seedlings were planted and screened for
583 heteroplasmy. Both F1 and F2 seedlings were genotyped at the *MSH1* locus as described in
584 Wu *et al.* 2020 (48). F2 plants that were homozygous for the *msh1* mutant allele were removed
585 from subsequent analyses.

586

587 **Acknowledgements:**

588 This work was supported by a grant from the National Institutes of Health (R01 GM118046 to
589 DBS). This project has received funding from the European Research Council (ERC) under the
590 European Union's Horizon 2020 research and innovation programme (Grant agreement No.
591 805046 (EvoConBiO) to IGJ).

592

593

594 **Author contributions:**

595 AKB: Conceptualization, Investigation, Formal analysis, Validation, Visualization, Writing –
596 Original Draft Preparation, Writing – Review and Editing

597 LK: Investigation, Formal analysis, Validation, Writing – Review and Editing

598 MFG: Investigation, Formal analysis, Writing – Review and Editing

599 MH: Investigation, Writing – Review and Editing

600 IGJ: Formal analysis, Funding Acquisition, Validation, Visualization, Writing – Review and
601 Editing

602 DBS: Conceptualization, Formal analysis, Funding Acquisition, Visualization, Writing – Original
603 Draft Preparation, Writing – Review and Editing

604

605

606 **Supporting Information:**

607 Figure S1. MSH1 does not significantly alter organellar genome copy number.

608 Figure S2. Organellar genome copy number varies within and between tissues.

609 Table S1. Distribution of SNVs over multiple generations of *msh1* mutant lines.

610 Table S2. Values of heteroplasmy for mother and progeny.

611 Table S3. Within plant heteroplasmy.

612 Table S4. Distribution of SNVs over two generations in wild type background.

613 Table S5. GC bias.

614 Table S6. Primers for ddPCR heteroplasmy assays and genome copy analysis.

615 Table S7. Allele-specific probes for ddPCR heteroplasmy assays.

Supporting information:

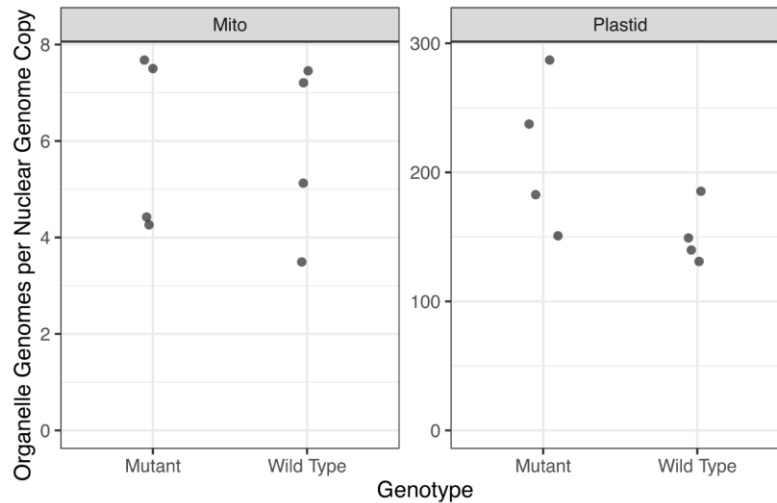


Figure S1. *MSH1* does not significantly alter organellar genome copy number. The number of mitochondrial and plastid genome copies per nuclear genome copy was determined using ddPCR, corrected for numts and compared between *msh1* mutant lines ($n = 4$) and wild type plants ($n = 4$). Organellar genome copies between mutant and wild type lines were not significantly different (mitochondria, $p = 0.910$; plastid, $p = 0.098$).

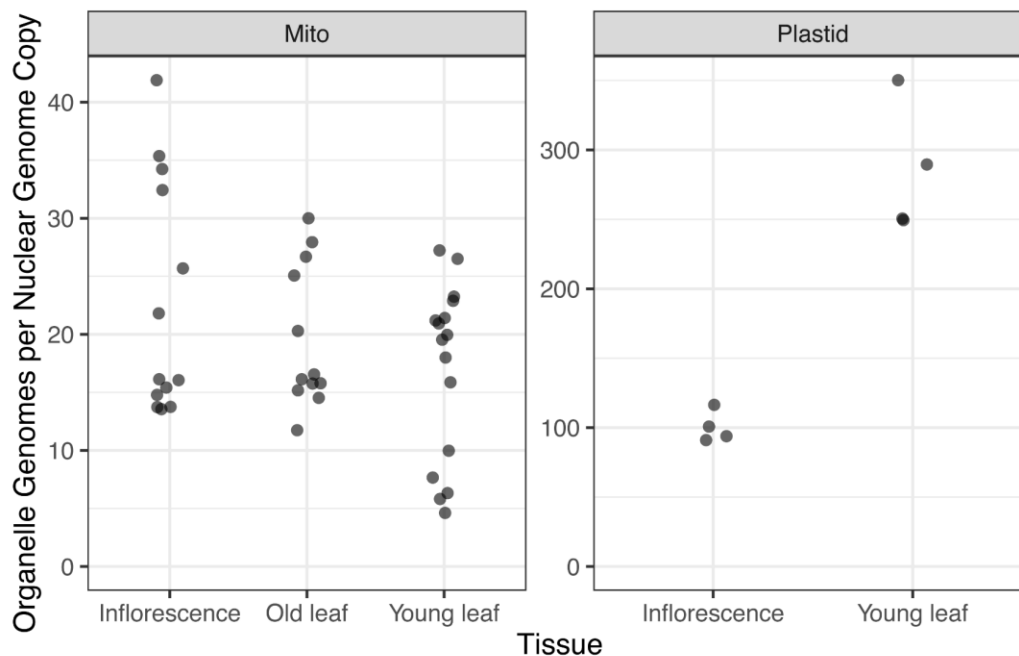


Figure S2. Organellar genome copy number varies within and between tissues. The number of mitochondrial and plastid genome copies per nuclear genome copy was determined using ddPCR and corrected for numts. For mitochondrial primers, tissue samples consisted of whole inflorescences ($n = 13$), old leaves harvested from the base of the rosette ($n = 12$), and young leaves harvested from the top of the rosette ($n = 16$). A subset of samples was chosen for analysis using plastid primers (inflorescences, $n = 6$; young leaf, $n = 6$). Plastid copies were significantly lower in inflorescences versus leaves ($p = 0.00028$); mitochondrial copies were not significantly different between tissue types. Mitochondrial values were adjusted for numt copies.

References:

- 616 1. C. V. Pereira, B. L. Gitschlag, M. R. Patel, Cellular mechanisms of mtDNA heteroplasmy
617 dynamics. *Critical reviews in biochemistry and molecular biology* **56**, 510-525 (2021).
- 618 2. J. C. Havird *et al.*, Selfish Mitonuclear Conflict. *Curr Biol* **29**, R496-r511 (2019).
- 619 3. J. Sobanski *et al.*, Chloroplast competition is controlled by lipid biosynthesis in evening
620 primroses. *Proceedings of the National Academy of Sciences* **116**, 5665-5674 (2019).
- 621 4. E. C. Røyrvik, I. G. Johnston, MtDNA sequence features associated with 'selfish
622 genomes' predict tissue-specific segregation and reversion. *Nucleic Acids Research* **48**,
623 8290-8301 (2020).
- 624 5. J. B. Stewart, P. F. Chinnery, The dynamics of mitochondrial DNA heteroplasmy:
625 implications for human health and disease. *Nat Rev Genet* **16**, 530-542 (2015).
- 626 6. H. A. Tuppen, E. L. Blakely, D. M. Turnbull, R. W. Taylor, Mitochondrial DNA mutations
627 and human disease. *Biochim Biophys Acta* **1797**, 113-128 (2010).
- 628 7. B. Arbeithuber *et al.*, Age-related accumulation of de novo mitochondrial mutations in
629 mammalian oocytes and somatic tissues. *PLoS Biol* **18**, e3000745 (2020).
- 630 8. J. B. Stewart, N. G. Larsson, Keeping mtDNA in shape between generations. *PLoS*
631 *Genet* **10**, e1004670 (2014).
- 632 9. I. G. Johnston *et al.*, Stochastic modelling, Bayesian inference, and new in vivo
633 measurements elucidate the debated mtDNA bottleneck mechanism. *Elife* **4**, e07464
634 (2015).
- 635 10. W. Wei *et al.*, Germline selection shapes human mitochondrial DNA diversity. *Science*
636 **364** (2019).
- 637 11. L. Cao *et al.*, New evidence confirms that the mitochondrial bottleneck is generated
638 without reduction of mitochondrial DNA content in early primordial germ cells of mice.
639 *PLoS Genet* **5**, e1000756 (2009).
- 640 12. T. Lieber, S. P. Jeedigunta, J. M. Palozzi, R. Lehmann, T. R. Hurd, Mitochondrial
641 fragmentation drives selective removal of deleterious mtDNA in the germline. *Nature*
642 **570**, 380-384 (2019).
- 643 13. T. Wai, D. Teoli, E. A. Shoubridge, The mitochondrial DNA genetic bottleneck results
644 from replication of a subpopulation of genomes. *Nature Genetics* **40**, 1484-1488 (2008).
- 645 14. I. G. Johnston, Varied Mechanisms and Models for the Varying Mitochondrial Bottleneck.
646 *Front Cell Dev Biol* **7**, 294 (2019).

- 647 15. C. W. Birky, The inheritance of genes in mitochondria and chloroplasts: Laws,
648 Mechanisms, and Models. *Annu Rev Genetics* **35**, 125-148 (2001).
- 649 16. M. Li *et al.*, Transmission of human mtDNA heteroplasmy in the Genome of the
650 Netherlands families: support for a variable-size bottleneck. *Genome Res* **26**, 417-426
651 (2016).
- 652 17. B. Rebolledo-Jaramillo *et al.*, Maternal age effect and severe germ-line bottleneck in the
653 inheritance of human mitochondrial DNA. *Proc Natl Acad Sci U S A* **111**, 15474-15479
654 (2014).
- 655 18. P. R. Wilton, A. Zaidi, K. Makova, R. Nielsen, A Population Phylogenetic View of
656 Mitochondrial Heteroplasmy. *Genetics* **208**, 1261-1274 (2018).
- 657 19. A. A. Zaidi *et al.*, Bottleneck and selection in the germline and maternal age influence
658 transmission of mitochondrial DNA in human pedigrees. *Proc Natl Acad Sci U S A* **116**,
659 25172-25178 (2019).
- 660 20. K. E. Bentley, J. R. Mandel, D. E. McCauley, Paternal leakage and heteroplasmy of
661 mitochondrial genomes in *Silene vulgaris*: evidence from experimental crosses. *Genetics*
662 **185**, 961-968 (2010).
- 663 21. J. R. Mandel *et al.*, Disentangling Complex Inheritance Patterns of Plant Organellar
664 Genomes: An Example From Carrot. *J Hered* **111**, 531-538 (2020).
- 665 22. D. E. McCauley, Paternal leakage, heteroplasmy, and the evolution of plant
666 mitochondrial genomes. *New Phytol* **200**, 966-977 (2013).
- 667 23. A. J. Ramsey, J. R. Mandel, "When One Genome Is Not Enough: Organellar
668 Heteroplasmy in Plants" in Annual Plant Reviews online. (2019),
669 10.1002/97811119312994.apr0616, pp. 619-658.
- 670 24. G. Drouin, H. Daoud, J. Xia, Relative rates of synonymous substitutions in the
671 mitochondrial, chloroplast and nuclear genomes of seed plants. *Mol Phylogenet Evol* **49**,
672 827-831 (2008).
- 673 25. D. R. Smith, Mutation rates in plastid genomes: they are lower than you might think.
674 *Genome Biol Evol* **7**, 1227-1234 (2015).
- 675 26. K. H. Wolfe, W. H. Li, P. M. Sharp, Rates of nucleotide substitution vary greatly among
676 plant mitochondrial, chloroplast, and nuclear DNAs. *Proc Natl Acad Sci U S A* **84**, 9054-
677 9058 (1987).
- 678 27. A. Massouh *et al.*, Spontaneous Chloroplast Mutants Mostly Occur by Replication
679 Slippage and Show a Biased Pattern in the Plastome of *Oenothera*. *Plant Cell* **28**, 911-
680 929 (2016).

- 681 28. S. Greiner, "Plastome Mutants of Higher Plants" in Genomics of Chloroplasts and
682 Mitochondria, R. Bock, V. Knoop, Eds. (Springer Netherlands, Dordrecht, 2012),
683 10.1007/978-94-007-2920-9_11, pp. 237-266.
- 684 29. H. J. Muller, The relation of recombination to mutational advance. *Mutat Res* **106**, 2-9
685 (1964).
- 686 30. J. Felsenstein, The evolutionary advantage of recombination. *Genetics* **78**, 737-756
687 (1974).
- 688 31. M. Unseld, J. R. Marienfeld, P. Brandt, A. Brennicke, The mitochondrial genome of
689 Arabidopsis thaliana contains 57 genes in 366,924 nucleotides. *Nature Genetics* **15**, 57-
690 61 (1997).
- 691 32. Q. Zhang, Y. Liu, Sodmergen, Examination of the Cytoplasmic DNA in Male
692 Reproductive Cells to Determine the Potential for Cytoplasmic Inheritance in 295
693 Angiosperm Species. *Plant and Cell Physiology* **44**, 941-951 (2003).
- 694 33. C. M. Barr, M. Neiman, D. R. Taylor, Inheritance and recombination of mitochondrial
695 genomes in plants, fungi and animals. *New Phytol* **168**, 39-50 (2005).
- 696 34. S. Greiner, J. Sobanski, R. Bock, Why are most organelle genomes transmitted
697 maternally? *Bioessays* **37**, 80-94 (2015).
- 698 35. J. R. Christie, M. Beekman, Uniparental Inheritance Promotes Adaptive Evolution in
699 Cytoplasmic Genomes. *Mol Biol Evol* **34**, 677-691 (2017).
- 700 36. J. R. Christie, M. Beekman, Selective sweeps of mitochondrial DNA can drive the
701 evolution of uniparental inheritance. *Evolution* **71**, 2090-2099 (2017).
- 702 37. D. M. Edwards *et al.*, Avoiding organelle mutational meltdown across eukaryotes with or
703 without a germline bottleneck. *PLoS Biol* **19**, e3001153 (2021).
- 704 38. A. L. Radzvilavicius, H. Kokko, J. R. Christie, Mitigating Mitochondrial Genome Erosion
705 Without Recombination. *Genetics* **207**, 1079-1088 (2017).
- 706 39. S. Greiner *et al.*, Chloroplast nucleoids are highly dynamic in ploidy, number, and
707 structure during angiosperm leaf development. *Plant J* **102**, 730-746 (2020).
- 708 40. L. Gao *et al.*, Changes in mitochondrial DNA levels during early embryogenesis in
709 *Torenia fournieri* and *Arabidopsis thaliana*. *Plant J* 10.1111/tpj.13987 (2018).
- 710 41. T. Preuten *et al.*, Fewer genes than organelles: extremely low and variable gene copy
711 numbers in mitochondria of somatic plant cells. *Plant J* **64**, 948-959 (2010).
- 712 42. D. Y. Wang *et al.*, The levels of male gametic mitochondrial DNA are highly regulated in
713 angiosperms with regard to mitochondrial inheritance. *Plant Cell* **22**, 2402-2416 (2010).

- 714 43. M. Woloszynska, Heteroplasmy and stoichiometric complexity of plant mitochondrial
715 genomes--though this be madness, yet there's method in't. *J Exp Bot* **61**, 657-671
716 (2010).
- 717 44. J. M. Gualberto, K. J. Newton, Plant Mitochondrial Genomes: Dynamics and
718 Mechanisms of Mutation. *Annu Rev Plant Biol* **68**, 225-252 (2017).
- 719 45. T. A. Ruhlman, J. Zhang, J. C. Blazier, J. S. M. Sabir, R. K. Jansen, Recombination-
720 dependent replication and gene conversion homogenize repeat sequences and diversify
721 plastid genome structure. *Am J Bot* **104**, 559-572 (2017).
- 722 46. H. Janska, R. Sarria, M. Woloszynska, M. Arrieta-Montiel, S. A. Mackenzie,
723 Stoichiometric shifts in the common bean mitochondrial genome leading to male sterility
724 and spontaneous reversion to fertility. *Plant Cell* **10**, 1163-1180 (1998).
- 725 47. X. Yang, S. A. Mackenzie, Many Facets of Dynamic Plasticity in Plants. *Cold Spring*
726 *Harb Perspect Biol* **11** (2019).
- 727 48. Z. Wu, G. Waneka, A. K. Broz, C. R. King, D. B. Sloan, MSH1 is required for
728 maintenance of the low mutation rates in plant mitochondrial and plastid genomes. *Proc*
729 *Natl Acad Sci U S A* **117**, 16448-16455 (2020).
- 730 49. J. I. Davila *et al.*, Double-strand break repair processes drive evolution of the
731 mitochondrial genome in Arabidopsis. *BMC Biol* **9**, 64 (2011).
- 732 50. R. V. Abdelnoor *et al.*, Substoichiometric shifting in the plant mitochondrial genome is
733 influenced by a gene homologous to MutS. *Proceedings of the National Academy of*
734 *Sciences* **100**, 5968-5973 (2003).
- 735 51. H. Ogata *et al.*, Two new subfamilies of DNA mismatch repair proteins (MutS)
736 specifically abundant in the marine environment. *ISME J* **5**, 1143-1151 (2011).
- 737 52. V. M. Ayala-García, N. Baruch-Torres, P. L. García-Medel, L. G. Brieba, Plant organellar
738 DNA polymerases paralogs exhibit dissimilar nucleotide incorporation fidelity. *Febs j*
739 **285**, 4005-4018 (2018).
- 740 53. A. C. Christensen, Genes and junk in plant mitochondria-repair mechanisms and
741 selection. *Genome Biol Evol* **6**, 1448-1453 (2014).
- 742 54. A. Marechal, N. Brisson, Recombination and the maintenance of plant organelle genome
743 stability. *New Phytol* **186**, 299-317 (2010).
- 744 55. P. Wonnapijit, P. F. Chinnery, D. C. Samuels, Previous estimates of mitochondrial DNA
745 mutation level variance did not account for sampling error: comparing the mtDNA
746 genetic bottleneck in mice and humans. *Am J Hum Genet* **86**, 540-550 (2010).
- 747 56. R. Lanfear, Do plants have a segregated germline? *PLoS Biol* **16**, e2005439 (2018).

- 748 57. A. L. Radzvilavicius, Z. Hadjivasiliou, A. Pomiankowski, N. Lane, Selection for
749 Mitochondrial Quality Drives Evolution of the Germline. *PLoS Biol* **14**, e2000410 (2016).
- 750 58. D. Smith, Updating Our View of Organelle Genome Nucleotide Landscape. *Frontiers in*
751 *Genetics* **3** (2012).
- 752 59. S. Xu *et al.*, High Mutation Rates in the Mitochondrial Genomes of *Daphnia pulex*.
753 *Molecular Biology and Evolution* **29**, 763-769 (2011).
- 754 60. B. Arbeithuber *et al.*, Advanced age increases frequencies of de novo mitochondrial
755 mutations in macaque oocytes and somatic tissues. *Proc Natl Acad Sci U S A* **119**,
756 e2118740119 (2022).
- 757 61. C. Haag-Liautard *et al.*, Direct estimation of the mitochondrial DNA mutation rate in
758 *Drosophila melanogaster*. *PLoS Biol* **6**, e204 (2008).
- 759 62. A. Konrad *et al.*, Mitochondrial Mutation Rate, Spectrum and Heteroplasmy in
760 *Caenorhabditis elegans* Spontaneous Mutation Accumulation Lines of Differing
761 Population Size. *Molecular Biology and Evolution* **34**, 1319-1334 (2017).
- 762 63. J. N. Wolff, D. J. White, M. Woodhams, H. E. White, N. J. Gemmell, The strength and
763 timing of the mitochondrial bottleneck in salmon suggests a conserved mechanism in
764 vertebrates. *PLoS One* **6**, e20522 (2011).
- 765 64. A. B. C. Otten *et al.*, Differences in Strength and Timing of the mtDNA Bottleneck
766 between Zebrafish Germline and Non-germline Cells. *Cell Reports* **16**, 622-630 (2016).
- 767 65. H. Zhang, S. P. Burr, P. F. Chinnery, The mitochondrial DNA genetic bottleneck:
768 inheritance and beyond. *Essays Biochem* **62**, 225-234 (2018).
- 769 66. L. M. Cree *et al.*, A reduction of mitochondrial DNA molecules during embryogenesis
770 explains the rapid segregation of genotypes. *Nat Genet* **40**, 249-254 (2008).
- 771 67. S. M. Bilinski, M. Kloc, W. Tworzydło, Selection of mitochondria in female germline cells:
772 is Balbiani body implicated in this process? *J Assist Reprod Genet* **34**, 1405-1412
773 (2017).
- 774 68. M. Colnaghi, A. Pomiankowski, N. Lane, The need for high-quality oocyte mitochondria
775 at extreme ploidy dictates mammalian germline development. *Elife* **10** (2021).
- 776 69. H. Zhang *et al.*, Mitochondrial DNA heteroplasmy is modulated during oocyte
777 development propagating mutation transmission. *Science Advances* **7**, eabi5657 (2021).
- 778 70. J. M. Watson *et al.*, Germline replications and somatic mutation accumulation are
779 independent of vegetative life span in *Arabidopsis*. *Proc Natl Acad Sci U S A* **113**,
780 12226-12231 (2016).

- 781 71. R. Hagemann, "Plastid Genetics in Higher Plants" in Cell Organelles, R. G. Herrmann,
782 Ed. (Springer Vienna, Vienna, 1992), 10.1007/978-3-7091-9138-5_2, pp. 65-96.
- 783 72. K. A. Lutz, Z. Svab, P. Maliga, Construction of marker-free transplastomic tobacco using
784 the Cre-loxP site-specific recombination system. *Nat Protoc* **1**, 900-910 (2006).
- 785 73. Z. Svab, P. Hajdukiewicz, P. Maliga, Stable transformation of plastids in higher plants.
786 *Proc Natl Acad Sci U S A* **87**, 8526-8530 (1990).
- 787 74. K. A. Lutz, P. Maliga, Plastid genomes in a regenerating tobacco shoot derive from a
788 small number of copies selected through a stochastic process. *Plant J* **56**, 975-983
789 (2008).
- 790 75. P. Maliga, R. Bock, Plastid Biotechnology: Food, Fuel, and Medicine for the 21st
791 Century. *Plant Physiology* **155**, 1501-1510 (2011).
- 792 76. Q. Rascón-Cruz *et al.*, Plastid transformation: Advances and challenges for its
793 implementation in agricultural crops. *Electronic Journal of Biotechnology* **51**, 95-109
794 (2021).
- 795 77. Y. Wang, Z. Wei, S. Xing, Stable plastid transformation of rice, a monocot cereal crop.
796 *Biochemical and Biophysical Research Communications* **503**, 2376-2379 (2018).
- 797 78. X. Liu, D. Weaver, O. Shirihai, G. Hajnóczky, Mitochondrial 'kiss-and-run': interplay
798 between mitochondrial motility and fusion–fission dynamics. *The EMBO journal* **28**,
799 3074-3089 (2009).
- 800 79. J. M. Segui-Simarro, M. J. Coronado, L. A. Staehelin, The mitochondrial cycle of
801 Arabidopsis shoot apical meristem and leaf primordium meristematic cells is defined by
802 a perinuclear tentaculate/cage-like mitochondrion. *Plant Physiol* **148**, 1380-1393 (2008).
- 803 80. R. J. Rose, Contribution of Massive Mitochondrial Fusion and Subsequent Fission in the
804 Plant Life Cycle to the Integrity of the Mitochondrion and Its Genome. *Int J Mol Sci* **22**
805 (2021).
- 806 81. J. M. Segui-Simarro, L. A. Staehelin, Mitochondrial reticulation in shoot apical meristem
807 cells of Arabidopsis provides a mechanism for homogenization of mtDNA prior to
808 gamete formation. *Plant Signal Behav* **4**, 168-171 (2009).
- 809 82. S. I. Arimura, Fission and Fusion of Plant Mitochondria, and Genome Maintenance.
810 *Plant Physiol* **176**, 152-161 (2018).
- 811 83. N. Galtier, The intriguing evolutionary dynamics of plant mitochondrial DNA. *BMC Biol* **9**,
812 61 (2011).
- 813 84. I. G. Johnston, Tension and Resolution: Dynamic, Evolving Populations of Organelle
814 Genomes within Plant Cells. *Mol Plant* **12**, 764-783 (2019).

- 815 85. J. M. Chustecki, R. D. Etherington, D. J. Gibbs, I. G. Johnston, Altered collective
816 mitochondrial dynamics in an *Arabidopsis msh1* mutant compromising organelle DNA
817 maintenance. *bioRxiv* 10.1101/2021.10.22.465420, 2021.2010.2022.465420 (2021).
- 818 86. S. Sato, Y. Nakamura, T. Kaneko, E. Asamizu, S. Tabata, Complete structure of the
819 chloroplast genome of *Arabidopsis thaliana*. *DNA research* **6**, 283-290 (1999).
- 820 87. R. Hershberg, D. A. Petrov, Evidence that mutation is universally biased towards AT in
821 bacteria. *PLoS Genet* **6**, e1001115 (2010).
- 822 88. F. Hildebrand, A. Meyer, A. Eyre-Walker, Evidence of selection upon genomic GC-
823 content in bacteria. *PLoS Genet* **6**, e1001107 (2010).
- 824 89. D. B. Sloan, Z. Wu, History of plastid DNA insertions reveals weak deletion and at
825 mutation biases in angiosperm mitochondrial genomes. *Genome Biol Evol* **6**, 3210-3221
826 (2014).
- 827 90. E. Pessia *et al.*, Evidence for widespread GC-biased gene conversion in eukaryotes.
828 *Genome Biol Evol* **4**, 675-682 (2012).
- 829 91. N. Galtier, L. Duret, Adaptation or biased gene conversion? Extending the null
830 hypothesis of molecular evolution. *Trends Genet* **23**, 273-277 (2007).
- 831 92. O. Khakhlova, R. Bock, Elimination of deleterious mutations in plastid genomes by gene
832 conversion. *Plant J* **46**, 85-94 (2006).
- 833 93. C.-S. Wu, S.-M. Chaw, Evolutionary Stasis in Cycad Plastomes and the First Case of
834 Plastome GC-Biased Gene Conversion. *Genome Biology and Evolution* **7**, 2000-2009
835 (2015).
- 836 94. Z. Niu *et al.*, Mutational Biases and GC-Biased Gene Conversion Affect GC Content in
837 the Plastomes of *Dendrobium* Genus. *International Journal of Molecular Sciences* **18**,
838 2307 (2017).
- 839 95. H. Ruwe, G. Wang, S. Gusewski, C. Schmitz-Linneweber, Systematic analysis of plant
840 mitochondrial and chloroplast small RNAs suggests organelle-specific mRNA
841 stabilization mechanisms. *Nucleic Acids Res* **44**, 7406-7417 (2016).
- 842 96. J. Forner, B. Weber, S. Thuss, S. Wildum, S. Binder, Mapping of mitochondrial mRNA
843 termini in *Arabidopsis thaliana*: t-elements contribute to 5' and 3' end formation. *Nucleic*
844 *Acids Res* **35**, 3676-3692 (2007).
- 845 97. Y. Yagi, T. Shiina, Recent advances in the study of chloroplast gene expression and its
846 evolution. *Frontiers in Plant Science* **5** (2014).

- 847 98. Z. Wu, J. D. Stone, H. Štorchová, D. B. Sloan, High transcript abundance, RNA editing,
848 and small RNAs in intergenic regions within the massive mitochondrial genome of the
849 angiosperm *Silene noctiflora*. *BMC Genomics* **16**, 938 (2015).
- 850 99. S. R. Kennedy *et al.*, Detecting ultralow-frequency mutations by Duplex Sequencing.
851 *Nature protocols* **9**, 2586-2606 (2014).
- 852 100. X. Zhang, R. Henriques, S. S. Lin, Q. W. Niu, N. H. Chua, Agrobacterium-mediated
853 transformation of *Arabidopsis thaliana* using the floral dip method. *Nat Protoc* **1**, 641-646
854 (2006).
- 855 101. M. Fernandes Gyorfy *et al.*, Nuclear-cytoplasmic balance: whole genome duplications
856 induce elevated organellar genome copy number. *Plant J* **108**, 219-230 (2021).
- 857 102. R. M. Stupar *et al.*, Complex mtDNA constitutes an approximate 620-kb insertion on
858 *Arabidopsis thaliana* chromosome 2: Implication of potential sequencing errors caused
859 by large-unit repeats. *Proceedings of the National Academy of Sciences* **98**, 5099
860 (2001).
- 861 103. X. Lin *et al.*, Sequence and analysis of chromosome 2 of the plant *Arabidopsis thaliana*.
862 *Nature* **402**, 761-768 (1999).
- 863 104. P. D. Fields *et al.*, Complete sequence of a 641-kb insertion of mitochondrial DNA in the
864 *Arabidopsis thaliana* nuclear genome. *bioRxiv* 10.1101/2022.02.22.481460,
865 2022.2002.2022.481460 (2022).
- 866 105. J. Nocedal, S. J. Wright, *Numerical optimization* (Springer, 1999).

